STONY BROOK UNIVERSITY

CEAS Technical Report 833

Joint Mobile Energy Replenishment and Data Gathering in Wireless Rechargeable Sensor Networks

Miao Zhao, Ji Li and Yuanyuan Yang

Department of Electrical and Computer Engineering

Stony Brook University

March 31, 2011

Joint Mobile Energy Replenishment and Data Gathering in Wireless Rechargeable Sensor Networks

Miao Zhao, Ji Li and Yuanyuan Yang

Department of Electrical and Computer Engineering, Stony Brook University, Stony Brook, NY 11794, USA

Abstract—Recent studies have shown that energy harvesting wireless sensor networks have the potential to provide perpetual network operations by capturing renewable energy from the external environment. However, the spatial-temporal profiles of such ambient energy sources typically exhibit great variations, and can only provide intermittent recharging opportunities for sensors to support low-rate data services. In order to provide steady and high recharging rates, and achieve energy-efficient data gatherings, in this paper we propose to utilize mobility for the joint design of energy replenishment and data gathering. In particular, a multi-functional mobile entity, called *SenCar* in this paper, is employed, which serves not only as a data collector that roams over the field to gather data via short-range communication but also as an energy transporter that charges static sensors on its migration tour via wireless energy transmissions. Taking advantages of the SenCar's controlled mobility, we give a two-step approach for the joint design. In the first step, the locations of a subset of sensors are periodically selected as *anchor points*, where the SenCar will sequentially visit to charge the sensors at these locations and gather data from nearby sensors in a multi-hop fashion. In order to achieve a desirable balance between the energy replenishment amount and data gathering latency, we provide a selection algorithm to search for a maximum number of anchor points where sensors hold the least battery energy, and meanwhile by visiting them the tour length of the SenCar is no more than a threshold. In the second step, we consider data gathering performance when the SenCar migrates among these anchor points. We formulate the problem into a network utility maximization problem and propose a distributed algorithm to adjust data rates, link scheduling and flow routing so as to adapt to the up-to-date energy replenishing status of sensors. The effectiveness of our approach is validated by extensive numerical results. When compared with solar harvesting networks, our solution can improve the network utility by 48% on the average.

Index Terms—Wireless rechargeable sensor networks, mobile energy replenishment, mobile data gathering, network utility.

I. Introduction

In recent years, energy harvesting technologies have been effectively integrated into wireless sensor systems. A variety of ambient energy, such as mechanical, thermal, photovoltaic, and electromagnetic energy can be converted into electrical energy to drive sensors or recharge sensor batteries, such that prolonged network lifetime or perpetual operations can be achieved [1][2]. However, as all these energy sources are from external environment and their spatial-temporal profiles exhibit great variations, the strength of harvested energy is typically low [3], and especially sensitive to the environment dynamics. For example, in a solar harvesting system, the output power of a sensor is determined by solar radiation arrives at the equipped solar panel, which drastically varies with time and weather. Statistics has shown that there is a difference of up to three orders of magnitude between the available solar power in cloudy, shadowy and sunny environments [4]. As there is generally lack of priori knowledge of the energy profile, such dynamics

imposes much difficulty on the design of protocols that must keep sensors from running out of energy. This is, however, very critical for many applications, especially environmental monitoring applications where the main task is to periodically collect data from all sensors. In case that some sensors deplete their energy and cannot get recharged in time, the network would ultimately become fragmented and the data from some parts of the sensing field can no longer be extracted.

In order to provide steady and high recharging rate for the power supplies of sensors, and meanwhile effectively alleviate energy expenditure on data gathering, in this paper we alternatively propose a joint design of energy replenishment and data gathering by exploiting mobility, which is referred to as J-MERDG. In particular, a multi-functional mobile entity, called *SenCar* in this paper, is employed, which is equipped with a powerful transceiver and high capacity battery. The SenCar will periodically choose a subset of sensors to visit. While migrating among these sensors, it delivers energy to the visited sensors by utilizing wireless energy transmissions and collects data from nearby sensors via short-range communication. This way, the SenCar, serving as both an energy transporter and a mobile data collector, performs the tasks of energy replenishment and data gathering simultaneously. In contrast to the conventional energy harvesting networks, the mobility brings us many benefits. First, since sensors receive energy supplement directly from the SenCar, the replenishment will no longer suffer from environmental variations. Second, as long as the SenCar moves close enough to sensors, high charging efficiency can be achieved to ensure high-rate data services. Third, as the SenCar takes the responsibility of energy delivery, it is commercially appealing that no complex energy harvesting devices are needed at each sensor, which significantly reduces the cost of entire network. Finally, by exploiting controlled mobility, the SenCar can efficiently perform energy delivery and data gathering simultaneously. This is extremely desirable as such combination makes double contribution to the energy management of the network. On one hand, the SenCar infuses steady and abundant renewable energy into the network almost at no additional cost. On the other hand, mobility alleviates the routing burden at sensors so that great energy can be saved to further leverage the refilled energy.

The objective of our work is to design an adaptive solution that jointly selects the sensors to be charged and finds the optimal data gathering scheme, such that network utility can be maximized while maintaining perpetual operations of the network. To that end, we propose a two-step approach for the joint design. In the first step, we determine the mobility pattern of the SenCar for each time period, i.e., where the SenCar will move to charge the sensors and gather the data from the neighborhood. For convenience, in this paper, we refer

to the locations that the SenCar visits as *anchor points*. In the second step, we focus on how to achieve the optimal data gathering performance when the SenCar migrates among the anchor points, considering the up-to-date energy replenishing status of sensors. We formulate this problem as an optimization problem and adjust data rates, link scheduling and flow routing to achieve maximum network utility.

The main contributions of our work can be summarized as follows.

- We propose a joint design of energy replenishment and data gathering (J-MERDG) by exploiting mobility. To the best of our knowledge, this is the first work that explores such joint design and systematically provides solutions to optimize its performance.
- We develop an algorithm for the SenCar to determine the anchor points in each time period, which achieves a desirable balance between the energy replenishing range and data gathering latency.
- We build a flow-level network maximization model to characterize the data gathering performance when the SenCar moves over different anchor points. We propose a proximal approximation based algorithm to obtain the system-wide optimum by adjusting data rates, link scheduling and flow routing in a distributed manner.
- We provide extensive numerical results to validate the effectiveness of J-MERDG, which not only guarantees perpetual operations of the network but also significantly outperforms solar harvesting system by 48% in network utility.

II. RELATED WORK

In this section, we briefly review some related work in the literature, which includes the work on energy replenishment in wireless networks, and the work on mobile data gathering in wireless sensor networks.

A. Energy Replenishment

Kar, et al. [6] considered a network with redundantly deployed rechargeable sensors, and addressed the problem of how sensors should be activated dynamically so as to maximize a global coverage metric. They proposed a threshold activation policy and demonstrated its performance for the cases that the coverage areas of sensors are completely or partially overlapped. Lin, et al. [7] developed a model to characterize the performance of multihop radio networks in the presence of energy replenishment and designed an energy-aware routing algorithm that is asymptotically optimal with respect to the network size. Liu, et al. [8] studied the resource allocation problem for energy-harvesting sensors. They first explored the optimal sampling rates based on the average (long term) energy replenishment rate and then designed a local algorithm for each sensor to adjust the rate according to the instantaneous battery state in order to cater to the recharging fluctuations. Sharma, et al. [9] presented a model for a single energy harvesting sensor node and identified two energy management policies for it. One policy is throughput-optimal, which ensures that the data queue stays stable for the highest possible data rate, and the other policy aims at minimizing the mean delay of the data queue.

Vigorito, et al. [10] considered the variability of the harvested environmental energy and designed an adaptive duty-cycling mechanism that achieves energy neutral operation, performance maximization and duty cycle stability. Rahimi, et al. [4] studied the feasibility of exploiting mobility to extend network lifetime, in which a small number of network nodes are autonomously mobile, allowing them to move in search of energy from the environment, recharge and deliver energy to immobile, energy-depleted nodes.

All the above works focus on energy harvesting networks and try to provide adaptive mechanisms to conquer the environment variations. Besides [4], other works did not consider exploiting mobility. Moreover, none of them combine the tasks of energy replenishment and data gathering and balance their performance. In contrast, by taking advantage of controlled mobility, our work jointly determines the sensors to be charged and computes the data rates, link activations and flow routes for mobile data gathering.

B. Mobile Data Gathering

It has been observed that sensors close to the static data sink deplete energy much faster than others due to the fact that they forward much more data than other sensors. Based on this observation, several researchers [11]-[17] have proposed to use the mobile data collector to achieve uniform energy consumption. Jea, et al. [12] proposed a scheme in which mobile collectors move along parallel straight lines for data collections. Wang, et al. [14] used mobile relays to help relieve sensors that are heavily burdened by a high volume of network traffic. They studied the performance of dense networks with a mobile relay node and showed that network lifetime is improved over a purely static network. Xing et al. [15] proposed a rendezvous design, which aims to find a set of rendezvous points (RPs) to be visited by the mobile collector within a required delay bound, while the network cost incurred in transmitting data from sources to RPs is minimized. Gatzianas and Georgiadis [17] presented a distributed maximum lifetime routing algorithm for sensor networks with a mobile base station, which considered both the energy and power constraints at each sensor. Miao and Yang [16] proposed a distributed algorithm to find optimal mobile data gathering strategies, which could guarantee the specified network lifetime and bounded data gathering latency.

Although aforementioned schemes can greatly save energy by utilizing mobile collectors compared to the relay routing in static networks, none of them has considered recharging the energy of network nodes. In contrast, our work explores the performance gain when recharging is possible. It computes the migration tour of the SenCar based on the joint consideration of recharging demand and data gathering performance, and also adapts adjustable system parameters to the up-to-date energy replenishing status to optimize the data gathering scheme.

III. PRELIMINARIES

In this section, we provide an overview on J-MERDG. The timing structure and the architecture of this joint design are illustrated in Fig. 1 and Fig. 2, respectively.

As each sensor has different energy status at different times, it is required for the SenCar to properly arrange which sensor gets
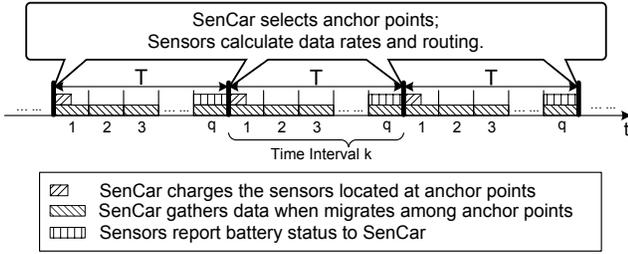
Fig. 1. Timing of joint mobile energy replenishment and data gathering (J-MERDG).
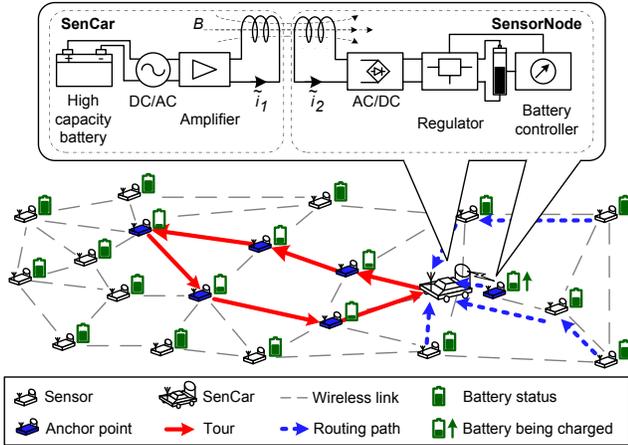
Fig. 2. Architecture of joint mobile energy replenishment and data gathering (J-MERDG).

recharged at what time. Due to such time-varying nature of the energy replenishment demand, to facilitate our study, we divide the time into fixed time intervals of length T. At the beginning of each time interval, the SenCar decides which sensors to be charged in this interval. We assume that the possible candidate locations for the SenCar to visit are the locations of all sensors, such that the SenCar can move sufficiently close to charge sensors with high efficiency. Based on some specified criteria (to be discussed in a subsequent section), the locations of a subset of sensors, i.e., anchor points, are selected. In this time interval, the sensors located at these anchor points would get recharged. As shown in Fig. 1, in each time interval, the SenCar will migrate among the anchor points back and forth. We assume that there are a total of q migration tours in each time interval. Along each tour, the SenCar would sojourn at each anchor point to gather data from nearby sensors via multi-hop communication. Without loss of generality, we assume that the SenCar sojourns for the same time at every anchor point in a tour. However, it should be pointed out that as anchor points in each time interval vary in quantity and positions, the sojourn time may be different from one time interval to another. During the last tour in a time interval, each sensor will report its up-to-date battery status to the SenCar. This information is transmitted piggyback with the data to the SenCar, which will be used for the anchor point selection at the beginning of next time interval.

While the SenCar arrives at an anchor point, it will quickly charge the sensor located there. The recharging structure is depicted in Fig. 2. The SenCar, as the energy transmitter, is equipped with a high-capacity rechargeable battery, a DC/AC converter and a resonant coil. For energy delivery, an oscillating

magnetic field is first induced around the transmitter coil on the SenCar. The sensor node, mounted with a receiver coil, is then tuned to resonate at exactly the same frequency, and use the AC/DC converter to generate DC current to recharge its battery. Such a structure is feasible and of high efficiency, which is supported by recent breakthroughs in two areas. The first area is the technology of highly-efficient wireless energy transmission, which was proposed for efficient non-radiative energy transmission over midrange [1]. The work in [18] and [19] has shown that through strongly coupled magnetic resonances, the efficiency of transferring 60 watts of power over a distance in excess of 2 meters is as high as 40%. Intel also demonstrated that it is possible to improve transferring 60 watts of power over a distance of up to two to three feet with efficiency of 75% [20]. At present, commercial products utilizing wireless energy transmission have been available on the market. The second area is the new battery material for ultra-fast charging. Ultra-fast charging was recently realized in $LiFePO_4$ by creating a fast ion-conducting surface phase through controlled off-stoichiometry [22]. It inherits and combines the advantages of both conventional Li-ion batteries and supercapacitors, which brings high energy density and can be charged at the rate as high as 400C [2]. Thus, this can shorten the time to fully charge a battery to few seconds.

While the SenCar arrives at an anchor point, it will also act as a data collector to gather the data from nearby sensors. Since the batteries can be charged in a very short time which can be almost neglected compare to the sojourn time, we assume that sensor batteries can be instantly fully-charged for use and the charging operation does not affect data gathering. In a particular time interval, as the SenCar moves over the anchor points in a tour, each sensor has the choice to send its data to the SenCar at any anchor point along low-cost routes. Moreover, in order to maximize network utility while maintaining perpetual operations, each sensor employs rate control to not only achieve high performance gain but also avoid draining out of energy before it can get recharged in a subsequent time interval. Next, we will present a carefully designed data gathering scheme that takes all these factors into consideration.

IV. JOINT MOBILE ENERGY REPLENISHMENT AND DATA GATHERING (J-MERDG)

Having outlined the basic idea of J-MERDG, in this section, we provide a two-step approach to efficiently implementing the design.

In the first step, the SenCar selects the anchor points for the current time interval by finding which sensors are to be recharged, where the SenCar will sojourn for data gathering, and how the SenCar moves over the field. In the second step, based on the information of SenCar's sojourn locations and the energy replenishing status, each sensor self determines how to transmit data to the SenCar when it arrives. The details of the approach are given in the following two subsections. Since

---

[1]Midrange refers to the distance between the transmitter and the receiver that is larger than the size of the devices by a factor of at least 2 to 3 [18].

[2]C is determined by the nominal capacity of the battery. For a battery with the capacity of 1000mAh, C=1000mA.

TABLE 1
ANCHOR POINT SELECTION ALGORITHM FOR TIME INTERVAL k

//$\mathcal{S}$ *is the set of sensors,* $\mathcal{B}_e^{(k-1)}$ *is the set of energy states of sensors*
at the end of time interval $k-1$, *and* L *is the tour length bound*
Input: $\mathcal{S} = \{1, 2, \ldots, N\}$, $\mathcal{B}_e^{(k-1)} = \{\check{b}_i^{(k-1)} | i \in \mathcal{S}\}$, and L
Output: Anchor point list $\mathcal{A}^{(k)}$ for time interval k
Sort the battery states in $\mathcal{B}_e^{(k-1)}$ in an increasing order and record the
result in another set $\mathcal{B}'$;
Map $\mathcal{S}$ to another set $\mathcal{S}'$ by rearranging the sensors in the sequence
corresponding to their respective battery states in $\mathcal{B}'$;
$u \leftarrow 1$; $v \leftarrow |\mathcal{S}'|$;
$m \leftarrow 0$; $p \leftarrow 0$;
while *true* **do**
    if $u > v$
        $p \leftarrow v$; break;
    end if
    $m = \lfloor \frac{1}{2}(u+v) \rfloor$;
    // *We use* $\mathcal{S}'(m)$ *to represent the* m_{th} *element in* $\mathcal{S}'$
    $\mathcal{A}^{(k)} \leftarrow \{\mathcal{S}'(1), \mathcal{S}'(2), \ldots, \mathcal{S}'(m)\}$;
    Find an approximate shortest tour among the anchor points in $\mathcal{A}^{(k)}$
    and denoted the result by TSP($\mathcal{A}^{(k)}$);
    case
        TSP($\mathcal{A}^{(k)}$) $< L$: $u \leftarrow m + 1$;
        TSP($\mathcal{A}^{(k)}$) $= L$: $p \leftarrow m$; break;
        TSP($\mathcal{A}^{(k)}$) $> L$: $v \leftarrow m - 1$;
    end case
end while
$\mathcal{A}^{(k)} \leftarrow \{\mathcal{S}'(1), \mathcal{S}'(2), \ldots, \mathcal{S}'(p)\}$;
Find an approximate shortest tour among the anchor points in $\mathcal{A}^{(k)}$;

(a) $L = 200m$. (b) $L = 300m$.

Fig. 3. An example to illustrate the selection algorithm to search for the anchor points in a time interval.

similar methods are adopted in different time intervals, in the following discussions, we will focus on a typical time interval.

A. Anchor Point Selection

Since energy replenishment and data gathering are jointly considered, the selection of anchor points falls into following two aspects. First, the senors located at the selected anchor points should be those with most urgent needs of energy supplement. Second, as the SenCar moves over the anchor points back and forth for data gatherings during a time interval, the length of each migration tour, which implies the data gathering latency, is expected to be short. To better enjoy the benefit of the energy supply provided by the SenCar, more anchor points should be selected such that more sensors can timely get recharged. However, this would adversely prolong the migration tour. Therefore, there is an inherent tradeoff between the number of sensors to be recharged and data gathering latency. Based on this observation, the anchor point selection problem for a particular time interval k can be described as follows. Given the up-to-date energy states of sensors obtained by the SenCar at the end of time interval $k-1$, find the maximum number of anchor points for time interval k such that the sensors located at these anchor points hold the least battery energy, and meanwhile by visiting these anchor points, the tour length of the SenCar is no more than a threshold.

Considering that the possible candidate anchor points are the locations of all the sensors, this problem is equivalent to finding a target sensor, by visiting the locations of all the sensors with the battery energy less than or equal to which, the length of shortest migration tour among them is bounded by the threshold. Motivated by this observation, we propose a selection algorithm to search for the anchor points with the pseudo code shown in Table 1. Given the set of sensors $\mathcal{S}$, the set of energy states of sensors at the end of the previous time interval $\mathcal{B}_e^{(k-1)}$, and the
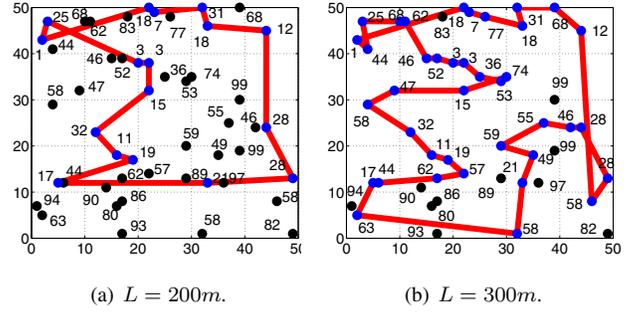
tour length bound L, the algorithm finds the anchor point list $\mathcal{A}^{(k)}$ for time interval k as follows.

As a pretreatment, the algorithm sorts the sensors with their battery energy in an increasing order. We record this sorted sensor list by $\mathcal{S}'$ and use $\mathcal{S}'(i)$ to represent the i_{th} element in the list. The problem is now converted to finding a target sensor $\mathcal{S}'(p)$ such that by visiting the senors with the index no more than p, i.e., $\mathcal{S}'(1), \mathcal{S}'(2), \ldots, \mathcal{S}'(p)$, the tour length is no more than L. To this end, the algorithm first finds the middle element of $\mathcal{S}'$, denoted by $\mathcal{S}'(m)$ and inspects the shortest migration tour among the locations of the sensors $\mathcal{S}'(1), \mathcal{S}'(2), \ldots, \mathcal{S}'(m)$. The migration tour can be found by an approximate solution to Traveling Salesman Problem (TSP). If the migration tour length equals the bound L, then the target sensor has been found; otherwise, the upper half or the lower half of the list is chosen to further search for the target sensor based on whether L is greater than or less than the migration tour among $\mathcal{S}'(1), \mathcal{S}'(2), \ldots, \mathcal{S}'(m)$. The algorithm reduces the number of elements needed to be checked to half each time, which is similar to the binary search algorithm [23]. We use $[u, v]$ to indicate the search range for the target sensor, where u and v are the indices of boundary elements. When there is no valid search range, i.e., $u > v$, it implies that there is no way to find a tour with the length exactly equal to L. Then, p is set by v and $\mathcal{S}'(p)$ is selected as the target sensor. By visiting the locations of $\mathcal{S}'(1), \mathcal{S}'(2), \ldots, \mathcal{S}'(p)$, the tour length will be closest to and less than L. It is clear that at most $\lceil \log(|\mathcal{S}|) \rceil$ rounds are needed to search for the target sensor. In each round, we need to calculate a tour among at most $|\mathcal{S}|$ sensors, which can be done in $O(|\mathcal{S}|^2)$ time. Therefore, the time complexity of the selection algorithm is $O(|\mathcal{S}|^2 \log(|\mathcal{S}|))$.

An example of the selection algorithm is illustrated in Fig. 3. There are 50 sensors in the network and their battery energy follows uniform distribution over $[0, 100]$. The nearest neighbor algorithm [23] for the TSP problem is used in our implementation to find the shortest tour among anchor points. The sensors on the migration tour are those to be charged in the current time interval. We can observe that regardless of the value of L, a higher precedence of sensors with lower energy are charged than other sensors. In addition, more sensors will be charged in the case of a larger L. For example, when $L = 200m$, 34% of the sensors, with the battery energy lower than or equal to 32, are charged and this results in a tour length of 193.2m. In contrast, when $L = 300m$, 78% of the sensors, with the battery energy lower than or equal to 77, are charged, which leads to a

tour length of 295.4m.

B. Optimal Mobile Data Gathering Scheme

After the anchor points are determined, the remaining work is how to gather the data from sensors when the SenCar migrates among the anchor points. We study such a mobile data gathering problem by formulating it into a utility maximization problem based on a flow-level network model. In the following, we first provide the problem formulation and then propose an optimization-based distributed algorithm for it.

1) Problem Formulation: For time interval k, consider a network with a set of static sensors, denoted by $\mathcal{S}$, and a set of anchor points, denoted by $\mathcal{A}^{(k)}$. To capture the characteristics of the SenCar movements over different anchor points in this time interval, we model the sensor network with the SenCar located at an anchor point a ($a \in \mathcal{A}^{(k)}$) by a directed acyclic graph $G_a^{(k)}(V_a^{(k)}, E_a^{(k)})$. $V_a^{(k)} = \mathcal{S} \bigcup \{\Lambda_a\}$ and represents the set of nodes, including all the sensors and the SenCar at anchor point a (denoted by Λ_a). $E_a^{(k)} = \{(i,j)|i, j \in V_a^{(k)}\}$, which is the set of directed links among the sensors and the SenCar. Sensor i generates data for the SenCar at a data rate of $r_{i,a}^{(k)}$ when the SenCar moves to anchor point a. The SenCar stays at each anchor point for a period of sojourn time $\tau^{(k)}$ in each of q tours in this time interval to collect data routed to it in multiple hops.

In our model, we use utility function $U_i(\cdot)$ to characterize the impact of the data from a sensor on the overall data gathering performance. We define $U_i(\cdot)$ as a strictly concave, increasing and twice-differentiable function with respect to the total amount of data gathered from sensor i in the current time interval (i.e., $\sum_{a \in \mathcal{A}^{(k)}} r_{i,a}^{(k)} q \tau^{(k)}$). Accordingly, the network utility is defined as the aggregation utility of all sensors. We are interested in maximizing the network utility while maintaining the perpetual operation of the network. To achieve this objective, we will address three critical issues: (1) what is the optimal data rate of a sensor for the SenCar sojourning at a particular anchor point; (2) how to schedule the link transmissions based on the interference model; (3) how to route the data to the SenCar at each anchor point taking into account of energy and link capacity constraints.

Now the mobile data gathering problem for time interval k can be formulated as follows. For clarity, all the notations used are summarized in Table 2.

$$\textbf{MDG:} \quad \max_{\mathbf{r}^{(k)}, \mathbf{f}^{(k)}} \sum_{i \in \mathcal{S}} U_i \left(\sum_{a \in \mathcal{A}^{(k)}} r_{i,a}^{(k)} q \tau^{(k)} \right) \quad (1)$$

Subject to

$$r_{i,a}^{(k)} + \sum_{j \in \mathcal{C}_{i,a}^{(k)}} f_{ji,a}^{(k)} = \sum_{j \in \mathcal{P}_{i,a}^{(k)}} f_{ij,a}^{(k)}, \forall i \in \mathcal{S}, \forall a \in \mathcal{A}^{(k)} \quad (2)$$

$$q \tau^{(k)} \sum_{a \in \mathcal{A}^{(k)}} \sum_{j \in \mathcal{P}_{i,a}^{(k)}} f_{ij,a}^{(k)} e_{ij} < \sigma b_i^{(k)}, \forall i \in \mathcal{S} \quad (3)$$

$$r_{i,a}^{(k)} \in R^+, f_{ij,a}^{(k)} \in \Pi_a^{(k)}, \forall i \in \mathcal{S}, \forall j \in \mathcal{P}_{i,a}^{(k)}, \forall a \in \mathcal{A}^{(k)} \quad (4)$$

where

$$b_i^{(k)} = \begin{cases} B_i, & \text{if } i \in \mathcal{A}^{(k)} \\ \check{b}_i^{(k-1)} & \text{otherwise} \end{cases} \quad \text{and} \quad \tau^{(k)} = \frac{T - q\text{TSP}(\mathcal{A}^{(k)})/v_s}{q|\mathcal{A}^{(k)}|} \quad (5)$$

TABLE 2
LIST OF NOTATIONS

Notation	Definition
$\mathcal{S}$	Set of sensors, i.e., $\mathcal{S} = \{1, 2, \ldots, N\}$
$\mathcal{B}^{(k)}$	Set of available battery energy of sensors for time interval k, i.e., $\mathcal{B}^{(k)} = \{b_i^{(k)}|i \in \mathcal{S}\}$
$\mathcal{B}_e^{(k)}$	Set of battery energy states of sensors at the end of time interval k, i.e., $\mathcal{B}_e^{(k)} = \{\check{b}_i^{(k)}|i \in \mathcal{S}\}$
B_i	Battery capacity of sensor i
$\mathcal{A}^{(k)}$	Set of anchor points for time interval k
$\mathcal{P}_{i,a}^{(k)}$	Set of parent nodes of sensor i for anchor point a in time interval k, i.e., $\mathcal{P}_{i,a}^{(k)} = \{j|(i,j) \in E_a^{(k)}\}$
$\mathcal{C}_{i,a}^{(k)}$	Set of child nodes of sensor i for anchor point a in time interval k, i.e., $\mathcal{C}_{i,a}^{(k)} = \{j|(j,i) \in E_a^{(k)}\}$
Λ_a	SenCar located at anchor point a
T	Length of each time interval
q	Number of migration tours in each time interval
L	Maximum migration tour length for SenCar
$\tau^{(k)}$	Sojourn time of SenCar at each anchor point in a migration tour during time interval k
$r_{i,a}^{(k)}$	Data rate of sensor i when SenCar sojourns at anchor point a during time interval k
$f_{ij,a}^{(k)}$	Flow rate over link (i,j) when SenCar is located at anchor point a in time interval k
$\Pi_a^{(k)}$	Feasible region of link capacity variable $f_{ij,a}^{(k)}$
σ	Portion parameter for the energy budget
e_{ij}	Energy consumed for transmitting a unit flow over link (i,j)
v_s	Moving velocity of the SenCar

The constraints can be explained as follows.

- Flow conservation constraint (2) states that at each sensor for each anchor point, the aggregated outgoing link flow rates equal the local data rate plus incoming link flow rates.
- Energy constraint (3) enforces the energy cost at each sensor in a time interval bounded by its energy budget, which is a portion of available battery energy.
- Capacity constraint (4) specifies that the capacity allocated on a link for a particular anchor point must fall in the feasible capacity region $\Pi_a^{(k)}$. Based on the node exclusive interference model in [26], $\Pi_a^{(k)}$ can be similarly defined as the convex hull of all the rate vectors of the matchings in $G_a^{(k)}$.

In the formulation, $b_i^{(k)}$ and $\tau^{(k)}$ represent the available battery energy of sensor i for time interval k and the sojourn time at each anchor point in a tour during time interval k, respectively. As the sensors located at anchor points can get fast recharging, they are considered to have the full battery energy for use, i.e., $b_i^{(k)} = B_i$, if $i \in \mathcal{A}^{(k)}$.

2) Distributed Algorithm for MDG Problem: It is observed that the objective function of MDG problem is concave, however, not strictly concave with respect to $r_{i,a}^{(k)}$. Directly solving it with the dual approach [25] may incur oscillation before the system enters the equilibrium, which is not amenable for practical implementations. Therefore, we resort to the proximal optimization algorithm [24], which can be explained as follows.

Proximal Approximation Based Algorithm: A quadratic term $-\frac{1}{2c}\|\mathbf{r}^{(k)} - \mathbf{x}^{(k)}\|_2^2 = -\frac{1}{2c} \sum_{i \in \mathcal{S}} \sum_{a \in \mathcal{A}^{(k)}} \left(r_{i,a}^{(k)} - x_{i,a}^{(k)} \right)^2$ is added to the original objective function to make it strictly concave, where $\mathbf{r}^{(k)} = \{r_{i,a}^{(k)}\}$, $\mathbf{x}^{(k)}$ is an additional matrix and c is a positive

scalar parameter. The proximal approximation algorithm runs in iterations, which alternatively maximizes the updated network utility over $\mathbf{r}^{(k)}$ while keeping $\mathbf{x}^{(k)}$ fixed, then over $\mathbf{x}^{(k)}$ while keeping $\mathbf{r}^{(k)}$ fixed, and repeats. In particular, the t_{th} iteration of the algorithm performs the following two steps.

Step 1: Fix $x_{i,a}^{(k)} = x_{i,a}^{(k)}[t]$ for all $i \in \mathcal{S}$ and $a \in \mathcal{A}^{(k)}$ and solve the following problem to obtain the optimal $r_{i,a}^{(k)}[t]$ and $f_{ij,a}^{(k)}[t]$.

$$\max_{\mathbf{r}^{(k)}, \mathbf{f}^{(k)}} \sum_{i \in \mathcal{S}} U_i \left(\sum_{a \in \mathcal{A}^{(k)}} r_{i,a}^{(k)} q\tau^{(k)} \right) - \frac{1}{2c} \|\mathbf{r}^{(k)} - \mathbf{x}^{(k)}\|_2^2 \quad (6)$$

subject to constraints (2), (3) and (4).

Step 2: Set $x_{i,a}^{(k)}[t+1] = r_{i,a}^{(k)}[t]$ for all $i \in \mathcal{S}$ and $a \in \mathcal{A}^{(k)}$.

Now, the remaining work is to solve problem (6). Since it is a strictly concave problem with respect to $\mathbf{r}^{(k)}$, we apply the subgradient method based on dual decomposition for it, which is an efficient technique for convex programs and can naturally achieve the distributed implementation.

Dual Decomposition: We relax constraint (2) by introducing Lagrangian multiplier $\lambda_{i,a}^{(k)}$. Then, we can obtain the partial Lagrangian

$$\begin{aligned} &L(\mathbf{r}^{(k)}, \mathbf{f}^{(k)}, \lambda^{(k)}) \\ &= \sum_i U_i(\sum_a r_{i,a}^{(k)} q\tau^{(k)}) - \frac{1}{2c} \cdot \sum_i \sum_a (r_{i,a}^{(k)} - x_{i,a}^{(k)})^2 \\ &\quad - \sum_i \sum_a \lambda_{i,a}^{(k)}(r_{i,a}^{(k)} + \sum_j f_{ji,a}^{(k)} - \sum_j f_{ij,a}^{(k)}) \\ &= [\sum_i U_i(\sum_a r_{i,a}^{(k)} q\tau^{(k)}) - \frac{1}{2c} \sum_i \sum_a (r_{i,a}^{(k)} - x_{i,a}^{(k)})^2 \\ &\quad - \sum_i \sum_a \lambda_{i,a}^{(k)} r_{i,a}^{(k)}] + \sum_i \sum_a \sum_j (\lambda_{i,a}^{(k)} - \lambda_{j,a}^{(k)}) f_{ij,a}^{(k)} \end{aligned} \quad (7)$$

By duality, the dual problem is therefore

$$\min_{\lambda^{(k)} \succeq 0} g(\lambda) = \min_{\lambda^{(k)} \succeq 0} \max_{\mathbf{r}^{(k)}, \mathbf{f}^{(k)}} L(\mathbf{r}^{(k)}, \mathbf{f}^{(k)}, \lambda^{(k)}) \quad (8)$$

Note that the dual problem has a good separable property, which can be decomposed into two subproblems. One is the rate control subproblem in terms of rate variables $\mathbf{r}^{(k)}$, and another is the joint scheduling and routing subproblem to find optimal flow variables $\mathbf{f}^{(k)}$.

a) **Rate Control Subproblem:** Given $\lambda_{i,a}^{(k)}$, each sensor solves a local optimization as follows by adjusting its data rates for different anchor points in time interval k.

$$\max_{r_{i,a}^{(k)} \geq 0} U_i(\sum_a r_{i,a}^{(k)} q\tau^{(k)}) - \frac{1}{2c} \sum_a (r_{i,a}^{(k)} - x_{i,a}^{(k)})^2 - \sum_a \lambda_{i,a}^{(k)} r_{i,a}^{(k)} \quad (9)$$

This local optimization can be solved by a similar approach to that in [27] with the complexity of $O(|\mathcal{A}^{(k)}| \log(|\mathcal{A}^{(k)}|))$, which is explained as follows.

Let μ_a be the Lagrangian multiplier for constraint $r_{i,a}^{(k)} \geq 0$. For each $a \in \mathcal{A}^{(k)}$, the Karush-Kuhn-Tucker conditions [25] are given by

$$\mu_a \geq 0, \quad (10)$$

$$\mu_a \cdot r_{i,a}^{(k)} = 0, \quad (11)$$

$$U_i'(\sum_a r_{i,a}^{(k)} q\tau^{(k)}) q\tau^{(k)} - \frac{1}{c} r_{i,a}^{(k)} + \frac{1}{c} x_{i,a}^{(k)} - \lambda_{i,a}^{(k)} + \mu_a = 0. \quad (12)$$

Let $m_{i,a}^{(k)} = \frac{1}{c} x_{i,a}^{(k)} - \lambda_{i,a}^{(k)}$. Then (12) can be rewritten as $U_i'(\sum_a r_{i,a}^{(k)} q\tau^{(k)}) q\tau^{(k)} - \frac{1}{c} r_{i,a}^{(k)} + m_{i,a}^{(k)} + \mu_a = 0$. If we sort the rates in the order that $m_{i,1}^{(k)} \geq m_{i,2}^{(k)} \geq \cdots \geq m_{i,|\mathcal{A}_i^{(k)}|}^{(k)}$, we

have that for any $1 \leq a' \leq a \leq |\mathcal{A}_i^{(k)}|$, $r_{i,a'}^{(k)} \geq r_{i,a}^{(k)}$. This result trivially holds when $r_{i,a}^{(k)} = 0$. And when $r_{i,a}^{(k)} > 0$, we have $\mu_a = 0$ and $r_{i,a'}^{(k)} - r_{i,a}^{(k)} = c(m_{i,a'}^{(k)} - m_{i,a}^{(k)}) + \mu_{a'} \geq 0$. Therefore, by using this result and the KKT conditions, there exists an A such that

$$r_{i,a}^{(k)} = \begin{cases} c\left[q\tau^{(k)} U_i'(R_i^{(k)} q\tau^{(k)}) + m_{i,a}^{(k)}\right] > 0, & a \leq A \\ 0, & a > A, \end{cases} \quad (13)$$

where $R_i^{(k)} = \sum_{a=1}^A r_{i,a}^{(k)}$ denotes the sum of data rates for different anchor points. This implies that to find the optimal value for every $r_{i,a}^{(k)}$, we only need to find optimal $R_i^{(k)}$ and the A.

When A is given, $R_i^{(k)}$ can be easily computed by solving the summation in (12) for all $a \leq A$. As $r_{i,a}^{(k)} > 0$ for all $a \leq A$, we have that $\mu_a = 0$ so that $R_i^{(k)}$ is the solution of $Aq\tau^{(k)} \cdot U_i'(R_i^{(k)} q\tau^{(k)}) - \frac{1}{c} R_i^{(k)} + \sum_{a=1}^A m_{i,a}^{(k)} = 0$. This way, all the work now becomes finding a proper A. As $r_{i,a}^{(k)}$ is decreasing in a and A is the boundary to indicate whether the rate is greater than or equal to zero, we search for A from $|\mathcal{A}_i^{(k)}|$ down to 1, and when $r_{i,A}^{(k)} = c\left[q\tau^{(k)} U_i'(R_i^{(k)} q\tau^{(k)}) + m_{i,A}^{(k)}\right] \geq 0$, we say A is found.

Finally, we summarize the rate control algorithm for subproblem (9) in Table 3.

TABLE 3
DISTRIBUTED RATE CONTROL ALGORITHM AT SENSOR i

Sort anchor points in $\mathcal{A}^{(k)}$ such that $m_{i,a}^{(k)}$ is in the decreasing order;
$A \leftarrow |\mathcal{A}^{(k)}|$;
$M \leftarrow \sum_{a=1}^{|\mathcal{A}^{(k)}|} m_{i,a}^{(k)}$;
While $A \geq 1$ **do**
    // Use $R_i^{(k)}$ to denote $\sum_{a=1}^A r_{i,a}^{(k)}$
    Solve $Aq\tau^{(k)} \cdot U_i'(R_i^{(k)} q\tau^{(k)}) - \frac{1}{c} R + M = 0$ for optimal $R_i^{(k)}$;
    Compute $r_{i,A}^{(k)} = c\left[q\tau^{(k)} U_i'(R_i^{(k)} q\tau^{(k)}) + m_{i,A}^{(k)}\right]$;
    If $r_{i,A}^{(k)} \geq 0$
        Compute the data rate for each anchor point as
        $r_{i,a}^{(k)} = \begin{cases} c\left[q\tau^{(k)} U_i'(R_i^{(k)} q\tau^{(k)}) + m_{i,a}^{(k)}\right] & a \leq A \\ 0 & a > A \end{cases}$;
        Break;
    else
        $M \leftarrow M - m_{i,A}^{(k)}$;
        $A \leftarrow A - 1$;
    end If
end While

b) **Joint Scheduling and Routing Subproblem:** Given $\lambda_{i,a}^{(k)}$, the how to schedule the link activation and how to allocate the flow rate on each scheduled link can be determined by solving the following subproblem.

$$\begin{aligned} \max \quad & \sum_i \sum_a \sum_j (\lambda_{i,a}^{(k)} - \lambda_{j,a}^{(k)}) f_{ij,a}^{(k)} \\ \text{s.t.} \quad & q\tau^{(k)} \cdot \sum_a \sum_j f_{ij,a}^{(k)} e_{ij} < \sigma b_i^{(k)}, \forall i \in \mathcal{S} \\ & f_{ij,a}^{(k)} \in \Pi_a^{(k)}, \forall i \in \mathcal{S}, \forall j \in \mathcal{P}_{i,a}^{(k)}, \forall a \in \mathcal{A}^{(k)} \end{aligned} \quad (14)$$

We first ignore the energy constraint when consider the link schedule, i.e., for each anchor point a, choose $\tilde{f}_{ij,a}^{(k)}$ such that

$$\tilde{f}_{ij,a}^{(k)} \in \arg \max_{f_{ij,a}^{(k)} \in \Pi_a^{(k)}} \sum_i \sum_j (\lambda_{i,a}^{(k)} - \lambda_{j,a}^{(k)}) f_{ij,a}^{(k)} \quad (15)$$

If we consider $\lambda_{i,a}^{(k)} - \lambda_{j,a}^{(k)}$ as the weight of link (i,j) destined for the SenCar at anchor point a, this scheduling problem is equivalent to the maximum weighted matching problem under the node exclusive interference model. We can utilize the heuristic distributed algorithms in [26] and [28] to solve this problem in $O(|E_a^{(k)}|)$ time.

Then problem (14) is reduced to a routing problem that determines how much flow rate on each link based on the schedule and energy constraints. Each sensor only needs to solve the following local problem

$$
\begin{aligned}
\max \quad & \sum_a \sum_j (\lambda_{i,a}^{(k)} - \lambda_{j,a}^{(k)}) f_{ij,a}^{(k)} \\
\text{s.t.} \quad & q\tau^{(k)} \cdot \sum_a \sum_j f_{ij,a}^{(k)} e_{ij} < \sigma b_i^{(k)} \\
& f_{ij,a}^{(k)} \le \tilde{f}_{ij,a}^{(k)}, \forall j \in \mathcal{P}_{i,a}^{(k)}, \forall a \in \mathcal{A}^{(k)},
\end{aligned}
\tag{16}
$$

where each $\tilde{f}_{ij,a}^{(k)}$ can be considered as the link capacity based on a specified schedule. This routing problem can be easily solved by an algorithm described in Table 4. The basic idea of the algorithm can be intuitively explained as follows. Each sensor always allocates a maximum flow rate under the energy and link capacity constraints to a scheduled link that has the largest link gain among all its outgoing links to different anchor points. Apparently, in the worst case, each sensor needs to consider the link gains of all its outgoing links for different anchor points. Thus, the time complexity of the routing algorithm at sensor i is $O(\sum_{a \in \mathcal{A}^{(k)}} \deg_a^+(i))$, where $\deg_a^+(i)$ is the outdegree of sensor i in the directed acyclic graph $G_a^{(k)}(V_a^{(k)}, E_a^{(k)})$.

TABLE 4
DISTRIBUTED ROUTING ALGORITHM AT SENSOR i

Set $f_{ij,a}^{(k)}$ to zero, for all $j \in P_{i,a}^{(k)}$, $a \in \mathcal{A}^{(k)}$;
Set $\mathbf{W}_i = \left\{ \lambda_{i,a}^{(k)} - \lambda_{j,a}^{(k)} > 0 \,\middle|\, \forall j \in P_{i,a}^{(k)}, \forall a \in \mathcal{A}^{(k)} \right\}$ and sort it in the decreasing order;
Initialize the battery energy for allocation: $b_r = \sigma b_i^{(k)}$;
For $iter = 1; iter <= |P_{i,a}^{(k)}| \cdot |\mathcal{A}^{(k)}|; iter{+}{+}$
  If $\mathbf{W}_i = \Phi$ or $b_r = 0$
    Break;
  end If
  $(\tilde{j}, \tilde{a})_i \leftarrow \underset{(j,a)}{\arg} \mathbf{W}_i[iter]$;
  $f_{i\tilde{j},\tilde{a}}^{(k)} = \min \left\{ \frac{b_r}{q\tau^{(k)} e_{i\tilde{j}}}, \tilde{f}_{i\tilde{j},\tilde{a}}^{(k)} \right\}$;
  Remove $\mathbf{W}_i[iter]$ from $\mathbf{W}_i$;
  $b_r \leftarrow b_r - q\tau^{(k)} f_{i\tilde{j},\tilde{a}}^{(k)} e_{i\tilde{j}}$;
end For

c) Lagrangian Multiplier Update: In each iteration of the subgradient algorithm, sensor i solves the subproblems in (9) and (14) with the current Lagrangian multiplier $\lambda_{i,a}^{(k)}[n]$. Then, sensor i updates the Lagrangian multipliers as follows and sends them to its direct neighbors to facilitate the computing of $r^{(k)}$ and $f^{(k)}$ in the next iteration.

$$
\begin{aligned}
\lambda_{i,a}^{(k)}[n+1] = & \\
& \left[\lambda_{i,a}^{(k)}[n] + \theta[n] \left(r_{i,a}^{(k)}[n] + \sum_j f_{ji,a}^{(k)}[n] - \sum_j f_{ij,a}^{(k)}[n] \right) \right]^+
\end{aligned}
\tag{17}
$$

where $[\cdot]^+$ denotes the projection onto the non-negative orthant and $\theta[n]$ is a properly chosen scalar stepsize for subgradient iteration n. In our algorithm, we choose the diminishing stepsizes, i.e., $\theta[n] = d/(b+ck), \forall k, c, d > 0, b \ge 0$, where b, c

and d are adjustable parameters that regulate the convergence speed. The diminishing stepsize can guarantee the convergence regardless of the initial value of λ [25].

d) Recovery of Primal Solutions: Since the subproblem of joint scheduling and routing is linear, which implies that the values in the optimal solution of the Lagrangian dual cannot be directly applied to the primal problem. In view of this, we apply the method introduced in [29] to recover the optimal primal values for variables $f_{ij,a}^{(k)}$. When the variables $x_{i,a}^{(k)}$ converge in the higher level optimization, during the subgradient iterations in the lower level we construct the primal feasible sequences $\{\hat{f}_{ij,a}^{(k)}[n]\}$ as follows.

$$
\begin{aligned}
\hat{f}_{ij,a}^{(k)}[n] &= \frac{1}{n} \sum_{h=1}^n f_{ij,a}^{(k)}[h] \\
&= \begin{cases} f_{ij,a}^{(k)}[1] & n = 1 \\ \frac{n-1}{n} \hat{f}_{ij,a}^{(k)}[n-1] + \frac{1}{n} f_{ij,a}^{(k)}[n] & n > 1 \end{cases}
\end{aligned}
\tag{18}
$$

Sherali and Choi [29] have proved that when the diminishing stepsize is used, any accumulation point of the recovered sequence generated by the method in (18) is feasible to the primal problem and it can converge to a primal optimal solution. Thus, optimal flow rates can be obtained when $\{\hat{f}_{ij,a}^{(k)}\}$ converges to $\hat{f}_{ij,a}^{(k)}{}^*$.

Finally, we summarize the proximal approximation based algorithm in Table 5, which is described in the context of sensor i for time interval k. As it is performed by each sensor and the information is only exchanged among direct neighbors, the algorithm is in a fully distributed manner.

TABLE 5
SUMMARY OF PROXIMAL APPROXIMATION BASED ALGORITHM

Initialize $\mathbf{x}_i^{(k)} = \{x_{i,a}^{(k)} | a \in \mathcal{A}^{(k)}\}$ to non-negative values;
// iterations for proximal approximation
Repeat
  Initialize Lagrangian multipliers $\lambda_i^{(k)} = \{\lambda_{i,a}^{(k)} | a \in \mathcal{A}^{(k)}\}$ to non-negative values;
  // iterations for subgradient and dual decomposition for (6)
  Repeat
    Compute $\mathbf{r}_i^{(k)}[n] = \{r_{i,a}^{(k)}[n] | a \in \mathcal{A}^{(k)}\}$ by solving rate control subproblem (9);
    Compute $\mathbf{f}_i^{(k)}[n] = \{f_{ij,a}^{(k)}[n] | j \in \mathcal{P}_{i,a}^{(k)}, a \in \mathcal{A}^{(k)}\}$ by solving joint scheduling and routing subproblem (14);
    Update lagrangian multiplier and send them to direct neighbors;
    If $\mathbf{x}_i^{(k)}$ get converged in the high-level proximal iterations
      Compute primal feasible $\hat{f}_{ij,a}^{(k)}[n]$ by (18);
    end If
  Until $\lambda_i^{(k)}$ and $\mathbf{r}_i^{(k)}$ converge;
  Set $\mathbf{x}_i^{(k)}[t+1] = \mathbf{r}_i^{(k)}[t]$ in the t_{th} proximal iteration;
Until $\mathbf{x}_i^{(k)}$ converges and get the final optimal $\mathbf{r}_i^{(k)}$ and $\mathbf{f}_i^{(k)}$

V. NUMERICAL RESULTS

In this section, we evaluate the effectiveness of J-MERDG with extensive numerical results, and compare it with the performance of the solar harvesting sensor system. In the evaluation, we use a network consisting of 10 wireless rechargeable sensors distributed over a 100m×100m area for demonstration purpose. In fact, due to the SenCar's capability of obtaining the sensor energy states along its migration tour and the distributed nature of the data gathering strategies, our design can be readily

TABLE 6
PARAMETER SETTINGS

Parameter	Value	Parameter	Value
B_i	2100mAh	e_{ij}	0.3mJ/Kbit
w_i	100	$e_{i\Lambda_i}$	0.02mJ/Kbit
$\theta(n)$	$\frac{1}{1+10n}$	L	200m
v_s	1m/s	σ	0.9
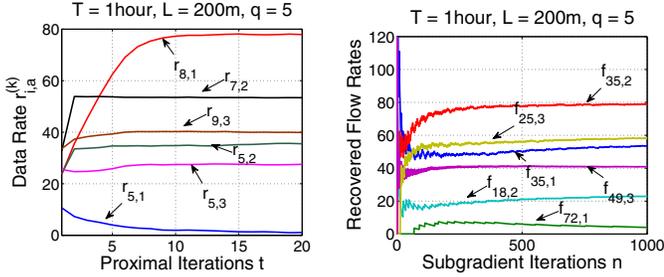
(a) Evolution of data rates versus proximal iterations t.

(b) Evolution of recovered flow rates versus subgradient iterations n.

Fig. 4. Convergence of the proximal approximation based algorithm.

(a) Cumulative network utility.

(b) Amount of gathered data in a tour.

(c) Number of recharged sensors.

(d) Sensor battery states.

Fig. 5. Performance of J-MERDG as the function of T.

applicable to large scale networks. The utility function $U_i(\cdot)$ is defined as $w_i \log(\sum_a r_{i,a}^{(k)} q\tau + 1)$, where w_i is the weight of utility at sensor i. If not specified otherwise, the time interval length T is set to one hour and the number of migration tours q in each time interval is equal to 5. For clarity, all other parameter settings are summarized in Table 6.

A. Convergence of Proximal Approximation Based Algorithm

We first examine the convergence of the proximal approximation based algorithm. For a particular time interval k, we assume that each sensor randomly holds 80%-100% of full battery capacity and the anchor points are set to the locations of sensors 1, 2 and 3. Fig. 4(a) shows the evolution of data rates $r_{i,a}^{(k)}$ versus the number of proximal iterations. It can be seen that all data rates approach to the stable status after only 10 iterations. Fig. 4(b) shows the evolution of recovered flow rates $\hat{f}_{ij,a}^{(k)}$ on some selected links versus the number of subgradient iterations. It is noticed that the recovered flow rates are well within 5% of their optimal values after only 500 iterations. To further dampen the number of subgradient iterations, which is the lower-level optimization of the proximal approximation based algorithm, we can set the initial values of Lagrangian multipliers $\lambda_{i,a}^{(k)}$ by their final values in the previous run of higher-level proximal iterations. Comparable performance can be observed when the number of subgradient iterations is as low as around 100.

B. Performance of J-MERDG

We now study the performance of J-MERDG varying with the time interval length T. Fig. 5(a) and 5(b) respectively demonstrate the evolution of cumulative network utility and cumulative number of recharged sensors in consecutive 24 hours under different settings of T. We assume that each sensor initially holds full battery capacity and the number of migration tours q in each time interval is proportional to T. From the figures, we can see that higher cumulative network utility can be obtained and there are more recharged sensors in the cases with a smaller T. This is reasonable since a smaller T leads to
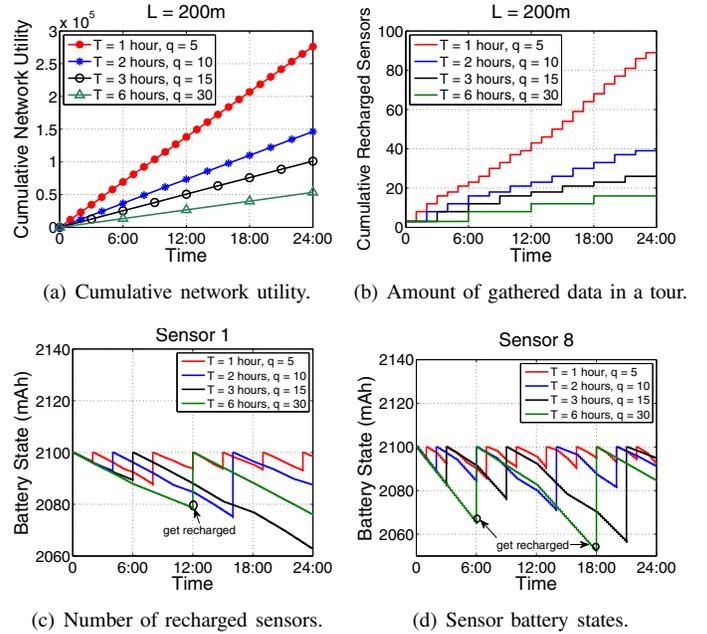
shorter waiting time for the sensors to get recharged. However, a small T may cause sensors to frequently calculate their data rates, schedule and routing so as to achieve the optimal data gatherings. Therefore, a proper setting for T is actually to balance the tradeoff between the computation overhead and achievable performance. Fig. 5(c) and 5(d) depict the battery states of sensor 1 and sensor 8 evolving with time, respectively. It is shown that sensors could timely get recharged to avoid energy depletion such that perpetual operations of the network can be guaranteed. It is apparent that sensors have more chances for energy replenishment under a smaller T. For example, sensor 8 is recharged for 9 times within 24 hours when $T = 1$ while it only gets recharged twice when $T = 6$.

C. Comparison with Solar Harvesting Sensor System

In this subsection, we compare J-MERDG with the mobile data gathering in the solar harvesting sensor system, denoted by MDG-SH for short. In MDG-SH scheme, each sensor harvests solar irradiance to self-support its energy consumption and a mobile collector visits each anchor point only for data gatherings. In order to sustain network operations, the energy consumption rate of each sensor can not be higher than the energy harvesting rate [8]. We build the recharging profiles of sensors for MDG-SH by using real solar irradiation measurements collected by the Baseline Measurement System (Global 40-South PSP) at National Renewable Energy Laboratory [30]. In particular, we first randomly choose 30 days of year 2009 and calculate the average irradiance of the sunny, cloudy and shadowy days based on the 30-day statistics, respectively. Then, the recharging rate can be derived as follows

$$\pi_r = \text{Rad}_s \times \eta_p \times \rho_e \times A, \qquad (19)$$

where Rad_s represents the solar irradiance, η_p is the efficiency of the solar panel to convert solar irradiance to electrical power, ρ_e is the electrical regulating and charging efficiency, and A is the size of solar panel. In our simulations, each sensor is

(a) Network utility.　(b) Amount of gathered data in a tour.
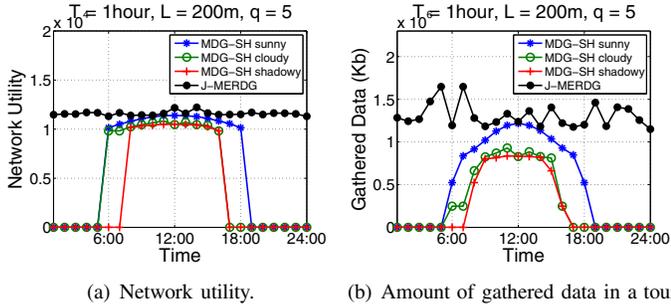
Fig. 6.　Performance comparisons between J-MERDG and MDG-SH.

assumed to have an equal recharging rate. And we set $\eta_p \times \rho_e$ to 0.06 and let A equal $37\text{mm} \times 37\text{mm}$.

Fig. 6 compares J-MERDG with MDG-SH in consecutive 24 hours in terms of network utility and the amount of gathered data. The amount of gathered data is used as one of the metrics because it more evidently visualizes the difference among different solutions than network utility, which is in logarithmic scale and results in a small slope at high data rates [8]. It is apparent in Fig. 6(a) that J-MERDG greatly outperforms MDG-SH all the time. On the average, J-MERDG achieves 48%, 59% and 66% higher network utility than MDG-SH in sunny, cloudy and shadowy days, respectively. These observations are also applicable to the amount of gathered data. It is shown in Fig. 6(b) that, during the day time (8:00-18:00), J-MERDG can collect 21%, 48% and 54% more data than MDG-SH in sunny, cloudy and shadowy days, respectively. Moreover, during night time, MDG-SH has no chance to harvest solar energy and thus cannot extract any data, while J-MERDG can still keep working and maintain the network utility as high as around 1.15×10^4. This fact signifies the importance of our work, which provides a recharging scheme immune to the environmental variations and also achieves high-performance data gathering.

VI. Conclusions

In this paper, we have studied the joint design of energy replenishment and data gathering (J-MERDG) in wireless sensor networks by exploiting mobility. Specifically, a SenCar is introduced to the wireless rechargeable sensor networks, which migrates among selected anchor points, charges the located sensors via wireless energy transmissions, and collects data from nearby sensors in multi-hop routing. In J-MERDG, we first presented a selection algorithm to determine the anchor points, which achieves a desirable balance between the energy replenishing amount and data gathering latency. Then, we explored the optimal data gathering performance when the SenCar moves over different anchor points. Each sensor self-tunes the data rate, scheduling, and routing based on the up-to-date energy replenishing status such that the entire network utility can be maximized. Numerical results demonstrated that J-MERDG can effectively maintain perpetual network operations and outperform solar harvesting systems by 48% in network utility.

References

[1] K. Lin, J. Yu, J. Hsu, S. Zahedi, D. Lee, J. Friedman, A. Kansal, V. Raghunathan and M. Srivastava, "Heliomote: enabling long-lived sensor networks through solar energy harvesting," *SenSys '05*, 2005.

[2] C. Park and P. Chou, "AmbiMax: autonomous energy harvesting platform for multi-supply wireless sensor nodes," *IEEE SECON ' 06*, 2006.

[3] S. J. Roundy, "Energy scavenging for wireless sensor nodes with a focus on vibration to electricity conversion," *Ph.D. Dissertation, Dept. of EECS, UC Berkeley*, May 2003.

[4] M. Rahimi, H. Shah, G. Sukhatme, J. Heideman and D. Estrin,"Studying the feasibility of energy harvesting in a mobile sensor network," *IEEE International Conference on Robotics and Automation*, 2003.

[5] T. Voigt, H. Ritter and J. Schiller, "Utilizing solar power in wireless sensor networks," *IEEE LCN '03*, pp. 416, 2003.

[6] K. Kar, A. Krishnamurthy and N. Jaggi, "Dynamic node activation in networks of rechargeable sensors," *IEEE/ACM Trans. Networking*, vol. 14, no. 1, pp. 15-26, Feb. 2006.

[7] L. Lin, N. B. Shroff and R. Srikant, "Asymptotically optimal energy-aware routing for multihop wireless networks with renewable energy sources," *IEEE/ACM Trans. Networking*, vol. 15, no. 5, pp. 1021-1034, Oct. 2007.

[8] R. S. Liu, P. Sinha and C. E. Koksal, "Joint energy management and resource allocation in rechargeable sensor networks," *IEEE INFOCOM '10*, March 2010.

[9] V. Sharma, U. Mukherji, V. Joseph and S. Gupta, "Optimal energy management policies for energy harvesting sensor nodes," *IEEE Trans. Wireless Communications*, vol. 9, no. 4, April 2010.

[10] C. Vigorito, D. Ganesan and A. Barto, "Adaptive control of duty cycling in energy-harvesting wireless sensor networks," *IEEE SECON '07*, 2007.

[11] R. Shah, S. Roy, S. Jain and W. Brunette, "Data mules: modeling a three-tier architecture for sparse sensor networks," *IEEE SNPA '03*, 2003.

[12] D. Jea, A. A. Somasundara and M. B. Srivastava, "Multiple controlled mobile elements (data mules) for data collection in sensor networks," *DCOSS '05*, 2005.

[13] J. Luo and J. P. Hubaux, "Joint mobility and routing for lifetime elongation in wireless sensor networks," *IEEE INFOCOM '05*, 2005.

[14] W. Wang, V. Srinivasan and K. Chua, "Extending the lifetime of wireless sensor networks through mobile relays," *IEEE/ACM Trans. Networking*, vol. 16, no. 5, pp. 1108-1120, 2008.

[15] G. Xing, T. Wang, W. Jia, and M. Li, "Rendezvous design algorithm for wireless sensor networks with a mobile base station," *ACM Mobihoc '08*, 2008.

[16] M. Zhao and Y. Yang, "An optimization based distributed algorithm for mobile data gathering in wireless sensor networks," *IEEE INFOCOM Mini-Conference*, 2010.

[17] M. Gatzianas and L. Georgiadis, "A distributed algorithm for maximum lifetime routing in sensor networks with mobile sink," *IEEE Trans. Wireless Communications*, vol. 7, no. 3, pp. 984-994, 2008.

[18] A. Kurs, A. Karalis, R. Moffatt, J. D. Joannopoulos, P. Fisher and M. Soljacic, "Wireless power transfer via strongly coupled magnetic resonances," *Science* vol. 317, pp. 83, 2007.

[19] A. Karalis, J. D. Joannopoulos and M. Soljacic, "Efficient wireless non-radiative mid-range energy transfer," *Annals of Physics*, vol. 323, no. 1, pp 34-48, Jan. 2008.

[20] Intel, "Wireless resonant energy link (WREL) demo," *http://software.intel.com/en-us/videos/wireless-resonant-energy-link-wrel-demo/*.

[21] S. Dearborn, "Charging Li-ion batteries for maximum run times," *Power Electronics Technology Mag.*, pp. 40-49, Apr. 2005.

[22] B. Kang and G. Ceder, "Battery materials for ultrafast charging and discharging," *Nature* 458, pp.190-193, March 2009.

[23] T. H. Cormen, C. E. Leiserson, R. L. Rivest and C. Stein, *Introduction to Algorithms*, MIT Press, 2001.

[24] D. Bertsekas and J. Tsitsiklis, *Parallel and Distributed Computation: Numerical Methods*, Athena Scientific, 1997.

[25] S. Boyd and L. Vandenbergh, *Convex Optimization*, Cambridge University Press, 2004. Available online: http://www.stanford.edu/ boyd/cvxbook/.

[26] L. Chen, S. H. Low, M. Chiang and J. C. Doyle, "Optimal cross-layer congestion control, routing, and scheduling design in ad hoc wireless networks," *IEEE INFOCOM '06*, 2006.

[27] X. Lin and N. B. Shroff, "Utility maximization for communication networks with multi-path routing," *Technical Report, Purdue Univ.*, 2004.

[28] U. Akyol, M. Andrews, P. Gupta, J. Hobby, I. Saniee and A. Stolyar, "Joint scheduling and congestion control in mobile ad-hoc networks," *IEEE INFOCOM '08*, 2008.

[29] H. Sherali and G. Choi, "Recovery of primal solutions when using subgradient optimization methods to solve Lagrangian duals of linear programs," *Operations Research Letters*, vol. 19, no. 3, pp. 105-113, 1996.

[30] National Renewable Energy Laboratory, http://www.nrel.org.